2014 IEEE International Conference on Robotics & Automation (ICRA)
Hong Kong Convention and Exhibition Center
May 31 - June 7, 2014. Hong Kong, China

Guidance of a High Dexterity Robot under 3D Ultrasound for Minimally Invasive Retrieval of Foreign Bodies from a Beating Heart

Paul Thienphrapa, Aleksandra Popovic, and Russell H. Taylor

***Abstract*— Particles such as thrombi, bullet fragments, and shrapnel can become trapped in a person's heart after migrating through the venous system, or by direct penetration. These cardiac foreign bodies pose a serious health risk as they can interfere with cardiovascular function. Conventional treatment often requires open heart surgery, cardiopulmonary bypass, and a long incision of the heart muscle, which come with significant risk and recovery time. To circumvent these disadvantages, we propose a minimally invasive surgical approach using 3D ultrasound to guide a dexterous robotic capture device.**

Analysis of the foreign body trajectory indicates highly erratic motion, rendering a robotic retrieval strategy based on direct pursuit of the tracked target infeasible. To provide a relatively slow robot with the ability to retrieve such a target, we propose alternative strategies based on guiding a robot to a salient capture location, and ambushing the target upon its reappearance. In this paper, we demonstrate the use of 3D transesophageal echocardiography (TEE) in tracking a foreign body in a beating heart phantom, computing a suitable capture location, and guiding a high dexterity robot to secure the target.

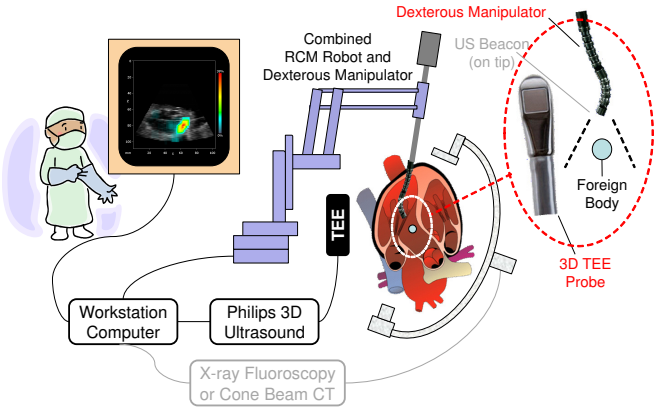

Fig. 1. Minimally invasive robotic retrieval of cardiac foreign bodies under 3D ultrasound guidance. Though not used in this study, CBCT integration is a future direction of interest.

I. Introduction

Foreign bodies introduced into the heart pose serious health risks, having the potential to cause arrhythmia, occlusion, neurotic manifestations, and even death [1], [2], in both civilian and military populations [3], [4]. Examples of cardiac foreign bodies include thrombi following myocardial infarction, small bullets and shell fragments that circulate freely in the chambers [1], [2], and other debris emerging from the venous system. Surgical treatment traditionally requires a median sternotomy followed by an incision in the pericardium [3], [5]–[7]. The procedure is highly invasive, involving long recovery periods and numerous health risks.

A minimally invasive operation on a beating heart can help mitigate the risks associated with sternotomy and cardiopulmonary bypass, and can potentially reduce procedure times. However, inhibited surgical access and visualization, and the motion of the foreign body in the heart, make the retrieval task difficult. To tackle these challenges, we proposed a procedure using a dexterous robotic device inserted transapically into the heart, and a 3D transesophageal echocardiography (TEE) probe to provide internal visualization. Under intraoperative 3D ultrasound guidance, the robot moves to secure the target, as illustrated in Fig. 1.

Manuscript received September 15, 2013 and revised January 22, 2014. This work was supported in part by Philips Research North America and in part by Johns Hopkins University internal funds.

Paul Thienphrapa and Russell H. Taylor are with the ERC CISST/LCSR, Johns Hopkins University, Baltimore, MD 21218, USA {pault,rht}@cs.jhu.edu.

Aleksandra Popovic is with Philips Research North America, Briarcliff Manor, NY 10510, USA aleksandra.popovic@philips.com.

In a previous study we tracked a foreign body in a beating heart phantom to characterize foreign body motion [8]. Then using an existing surgical robot, we demonstrated that the motion of the foreign body exceeds the ability of the robot to pursue it [9]. We thus introduced indirect capture strategies [8], [10] in which the moving target is ambushed rather than chased, thereby relaxing robot performance requirements.

In the present study we introduce a new dexterous minimally invasive surgical robot with 11 degrees of freedom (DOFs). We test our 3D TEE-based tracking and capture strategies in a live setting through experiments involving the retrieval of a foreign body from a beating heart phantom. A brief summary of the present system appears in an abstract [11]. The current paper presents the system in considerably more detail and includes new experimental results.

II. Related Work

Three-dimensional transthoracic echocardiography (TTE) is used to track a surgical instrument fitted with passive markers by Stoll *et al.* [12] with 1.0 mm of accuracy and a 2-Hz control rate. In subsequent experiments, similar results were obtained when targets were also tracked [13]. Liang *et al.* [14] performed needle-touch experiments with 1.2 mm of error; ultrasound targets were then embedded in chicken breast to mimic a breast biopsy procedure. In water tank experiments, the tracking error of a one-DOF heartbeat compensation device for mitral valve repair was found to be about 1.0 mm when using a predictive controller running at an 8-Hz control rate [15]. This work was extended to ultrasound servoing of a cardiac catheter [16].

Studies on ultrasound guidance have centered around 2D probes; nevertheless, the insights may abstract to 3D. For example, B-mode images of an object are referenced to a model object [17], [18] to reveal the pose of a robot-held probe. The known shapes of surgical tools can be leveraged in a similar fashion [19], [20]. Volumetric images can be constructed by sweeping a 2D probe [21], [22].

In a more tracking-focused study, a variable magnetic field was used to vibrate otherwise invisible ferrous targets, allowing for localization to within 1.1 mm [23]. This theme is retained in the use of piezoelectric buzzers to induce vibrations in a surgical tool [24].

Recent developments feature applications of 3D ultrasound in cardiac surgery. In the work of Moore *et al.* [25], 3D TEE is used for manual guidance of a novel cardiac surgical instrument. With a transesophageal probe tracked by an electromagnetic tracker, the surgeon identifies the mitral valve in the image, allowing the system to create an image overlay of the structure. The instrument position is also tracked and incorporated into an augmented reality view, helping the surgeon guide the instrument towards the mitral valve. In Gosline *et al.* [26], a surgeon uses 3D ultrasound to guide via teleoperation a concentric tube robot to place a patent foramen ovale closure device.

The work discussed herein bears some key distinctions from the aforementioned studies. The first is the 3D ultrasound-based guidance of a robot with distal dexterity, leading to enhanced workspace coverage inside the heart. This is in contrast to rigid instruments that rely predominantly on pivots about the surgical entry point (remote center of motion, or RCM); tools whose distal degree of freedom travels along its axis of insertion [15]; dexterous devices with motion constraints such as catheters [16] and concentric tubes [26]; and devices that are guided manually [25], [26]. Internal dexterity further implies that manipulation respecting the RCM point requires appropriate redundancy resolution, as opposed to the technique of mirroring motions about said point [13]. Another distinguishing factor relates to the proposed task, i.e., demonstration of 3D ultrasound in guiding a robot to capture an erratically moving target, in a dynamic environment. Finally, our 3D ultrasound control bandwidth of approximately 20 Hz is higher than previously reported for robot guidance, and is well suited for tasks of this nature, including tracking of the heart wall [27].

III. Review: Foreign Bodies in the Heart

This section reviews the findings of our previous efforts [8]–[10] in understanding foreign body behavior. Such knowledge is critical in moving forward with the design of a robotic system and capture strategies, so previous results are summarized here for context.

A. Tracking and Motion Characterization

In a precursor study [8], a 3.2-mm steel ball was inserted into the left ventricle of a beating heart phantom to mimic a clinical trauma case. The chosen stroke volume, about 18 ml, is lower than in healthy humans, reflecting surgical [28] and cardiovascular conditions following heart injury. Ultrasound volumes were acquired at rate of about 20 frames per second. Tracking of the foreign body was performed using 3D normalized cross-correlation (NCC), a commonly used template matching algorithm, with an RMS error of 2.3 mm. Despite occasional instances of loss of tracking, which were both detectable and recoverable, the benefits of this approach were its simple implementation and real-time computational performance.

The experiments revealed foreign body speeds of 343.5 mm/s, comparable to and in agreement with figures for the heart wall (300 mm/s [29]) and mitral valve (200 mm/s [15]). There was also a considerable amount of irregular motion, as indicated by significant frequency components of the motion above the 1-Hz heartbeats.

Despite the challenging robot performance requirements, a straightforward chasing experiment was nevertheless attempted using a low dexterity robot [9]. However, for the robot to reach the target to within a reasonable amount of error (2.1 mm), the speed of the virtual target had to be reduced by a factor of 9. This result highlights the need for robots with the distal dexterity to navigate the heart chamber. Even then, millimeter-level accuracy may be difficult to attain at speed, so careful planning may be preferred over direct pursuit.

B. Capture Locations

Chasing a foreign body inside a beating heart may be hazardous; as well, the foreign body exhibits a preference towards a subsection of the overall volume. These factors motivate a relaxed retrieval approach wherein the end effector is aimed at a location where likelihood of intercept is greatest. We previously outlined the following criteria for computing these capture locations [8], [10].

1) *Spatial probability*: Which locations are expected to contain the foreign body the most?
2) *Dwell time*: How long does the foreign body dwell in a certain location before it leaves? When it leaves, how long before it returns?
3) *Visit frequency*: How often does the foreign body visit, or traverse, a certain location?

In sum, the foreign body is in the most probable location 50.5% of the time, dwells in the most dwelled location for 0.84 seconds at a time, and visits the most visited location at a rate of 1.54 Hz. Fig. 2 shows a probability map for qualitative intuition. Red regions indicate where the foreign body is likely to be captured. In the envisioned operation, the system observes the fragment motion, computes a capture location in real time, and guides the robot to this location taking into consideration the probability of success, reachability, and manipulability.

IV. Robot System Description

The 11-DOF robot (Fig. 3) used in this study is a new system, composed of a new four-DOF snake robot (based on an existing design [30]–[34]) attached serially to an existing seven-DOF LARS robot [35]. The JHU snake robot,

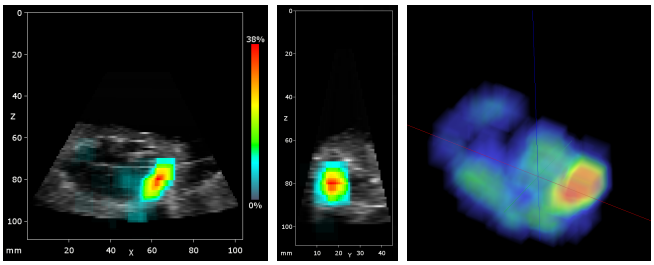

Fig. 2. Spatial probability map of the foreign body position. (*Left and center*) Coronal and sagittal slices. (*Right*) 3D view.

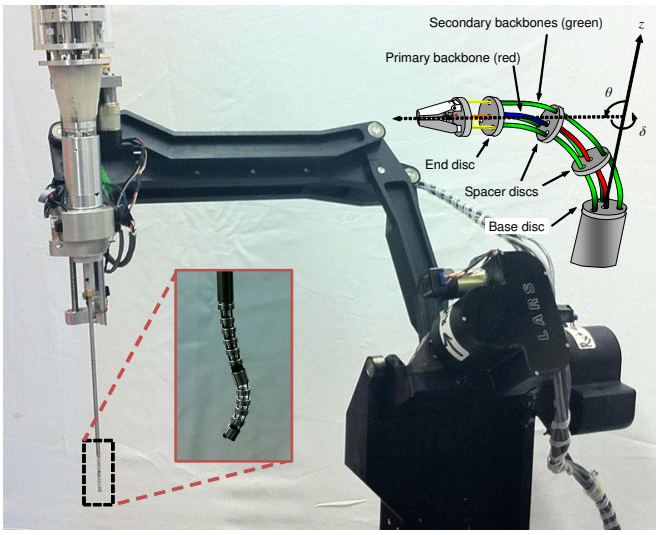

Fig. 3. The 11-DOF high dexterity robot, formed by a seven-DOF LARS robot holding a four-DOF snake robot. The snake robot consists of two two-DOF segments (the DOFs of each segment are shown in the drawing), giving rise to the S-bend capability shown in the inset.

originally designed for laryngeal surgery, features a small dexterous manipulator totaling 39.5 mm in length with a 4.2-mm diameter, appearing at the distal end of a 284.0-mm long stem. As shown in Fig. 3, the DOFs of each of the two serial snake segments include the angle of bend *from* the local z-axis (θ), and the angle of the bending plane *about* this z-axis (δ). The IBM/JHU LARS robot, meanwhile, was originally designed as a laparoscopic tool holder with three translational DOFs (X, Y, and Z), three rotational DOFs (RX, RY, and a θ about the tool axis), and an insertion DOF s along the tool axis.

The kinematic redundancy and dexterity offered by this union provides the flexibility to implement modes of control tailored to different parts of the procedure. The combination robot is abstracted as a single unit through a hybrid motion controller: a Galil DMC-4080 for the LARS and a custom FireWire-based device [36] for the snake. Software is based on the *cisst* libraries.

A. Robot Control

We are interested in resolving the spatial redundancy of the 11-DOF LARS-snake robot while satisfying task goals and respecting motion restrictions, whether in configuration space (joint limits) or the workspace (e.g. forbidden regions). These requirements can be formulated as an optimization problem [37]. A weighted constrained least squares optimization problem that solves for a set of joint increments Δq takes the form of (1). To produce robot motions ($J(q)\cdot\Delta q$) reflecting commanded ones (τ) within joint limits (q_{lower}, q_{upper}), we formulate objectives and constraints as follows.

$$\begin{aligned} \underset{\Delta q}{\text{minimize}} \quad & \|W\cdot(J(q)\cdot\Delta q-\tau)\| \\ \text{subject to} \quad & H\cdot\Delta q\geq h. \end{aligned} \tag{1}$$

$J(q)$ is the instantaneous Jacobian matrix relating the task and joint space velocities, $H=[I,-I]^T$, and $h=[(q_{lower}-q)-(q_{upper}-q)]$. W is a diagonal matrix specifying the weight of each degree of freedom. The robot motion is slow and approximately linear for small increments, so dynamic effects are excluded. Multiple objectives and constraints can be incorporated by concatenating the associated matrices.

Through adjustment of W in (1) [37], the optimization framework allows for various modes of operation as prescribed by application requirements. Coarse positioning can be achieved by assigning higher priorities to the LARS joints; this is useful, for example, in the initial robot placement. Fine positioning can be realized by preferring the snake joints. Furthermore, the dexterity of the snake can be augmented by some or all of the LARS joints.

The framework also enables the creation of virtual fixtures, such as a virtual RCM [38]. Upon a user-initiated transition to RCM mode, a fixed point on the snake stem is designated as the RCM. Constraints that restrict transverse motions from this point are then engaged.

A highly dexterous robot provides a number of benefits over straight tools, manual or robotic. An RCM limits the workspace of a straight tool, and the entry port itself may further reduce the workspace by restricting the available pivot range. With a dexterous tool, much of the mobility is transferred to the inside of the body, leading to enhanced workspace coverage while reducing the external motion envelope of the robot. Finally, robotic control is advantageous because high dexterity can be difficult to manage intuitively.

V. Experiments and Results

A. Experimental Setup

The setup for retrieval experiments is illustrated in Fig. 4. It consists of a beating heart phantom (Section III-A) to recreate the clinical scenario, an ultrasound system to image the scene, a high dexterity robot (Section IV) to capture the foreign body, and a PC for tracking and guidance.

The ultrasound system consists of a Philips iE33 xMATRIX Echocardiography System and an X7-2t 3D TEE probe. Volumes are streamed at about 20 frames per second over TCP/IP to the PC (2 GHz Xeon dual-core CPU, 4 GB of RAM) for processing and tracking. The image resolution is $176\times96\times176$, spanning a field of view of 60° azimuth, 30° elevation, and 12 cm depth. Gain and compression are set at 49% and 40 dB respectively.

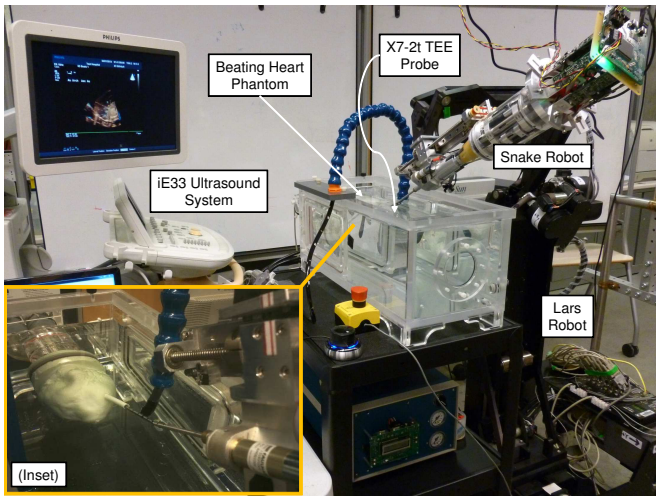

Fig. 4. Setup for 3D ultrasound (TEE) guidance experiments using a high dexterity robot to capture a foreign body in a beating heart phantom.

A small 1.6×3.2 mm magnet is affixed to the snake robot tip to act as an abstract capture device with high attractive force within the capture range and negligible effect beyond it. The magnet was tested by advancing it vertically downwards towards a foreign body resting in water. The attraction distance was found to be 4.2 mm over 20 repetitions. Although a different capture mechanism, such as suction, may have a more lenient capture range, dexterous targeting of the end effector remains important as it can help reduce perioperative time, improve capture certainty, and minimize blood loss over undirected suction.

B. Procedure

1) *Preoperative registration*: The robot is moved to various positions to generate a set of points in robot and image coordinate systems, from which a transformation matrix is computed. The fiducial registration error (FRE) was 1.1 mm, a reasonable result given the resolution of about 0.8 mm/pixel.
2) *RCM placement*: In coarse positioning mode, the robot is teleoperated to the surgical entry point at the apex of the heart phantom. The RCM is defined upon user-initiated switch to dexterous/RCM mode.
3) *Tracking initialization*: The foreign body is selected from ultrasound images of the heart phantom for use as a template to track the foreign body henceforth.
4) *Capture location computation*: The foreign body tracking loop is activated, and the tracked positions are used to compute a capture location in real time.
5) *Robot guidance*: Once a capture location is found, the robot is guided to capture the foreign body.

Under the spatial probability method, a capture location emerges once a probability reaches 50%; when using the dwell time approach, a peak measurement that is twice that of the runner up is used as the decision threshold. These values are inspired by findings from our previous work [39]. The visit rate method is not included in this set of experiments as it is more suited for a net-like mechanism that captures a target in transit. A capture is successful if the foreign body attaches to the magnetic tip without disengaging for at least five seconds, and unsuccessful if this condition is not met within 15 seconds of finding a capture location.

C. Success Rate

An example capture sequence is shown in Fig. 5. The system was able to retrieve the foreign body in 86.4% of attempts, including those based on spatial probability (14/17) and dwell time (5/5). Failed captures (13.6%) were due to the foreign body shifting after a capture location had been identified, but before the robot could reach it. This suggests that even a straightforward adjustment strategy, such as manual reset, can improve success rate. The 86.4% success rate for single-shot trials is thus encouraging.

Inspired by these findings, efforts on automatic repositioning are in progress. The first attempt uses the 15-second threshold to decide failure, but more advanced metrics such as expected waiting times may be used in the future. Preliminary findings suggest that 100% success is plausible.

D. Execution Times

Table I lists retrieval times broken down by phase. During observation, the system passively tracks the foreign body to compute a capture location. Because heart surgery can last several hours, an average observation time of 35.2 seconds suggests that more time can be afforded to improve results.

TABLE I
FOREIGN BODY RETRIEVAL EXECUTION TIMES (SECONDS)

	Type of Capture Location Used		
Phase	Probability	Dwell Time	Overall
Observation	29.6 ± 6.9	54.3 ± 33.1	35.2 ± 18.9
Insertion	2.8 ± 0.3	3.1 ± 0.5	2.9 ± 0.4
Waiting	3.7 ± 2.0	2.2 ± 1.5	3.3 ± 1.9
Total[1]	97.7 ± 21.6	124.5 ± 68.4	103.8 ± 37.1

[1] Includes retraction time

The insertion phase encapsulates the travel time of the robot, which was relatively consistent at 2.9 seconds throughout the experiments. The motion was slow enough to be monitored in the ultrasound stream, but not so much as to profoundly affect procedure times.

Upon reaching a capture location, the robot may need to wait for the foreign body to return; this waiting phase was found to last 3.3 seconds on average. It is possible that the foreign body will chance into capture after a sufficiently long wait. However, in placing the robot in non-capture locations, we did not observe such an event over runs of 4:44, 4:30, and 5:05 minutes. Such wait times may be difficult to tolerate, especially with a time-sensitive device such as suction.

The total times (Table I, *bottom row*) vary widely because retraction was commanded through user input. Nevertheless, retrieval times of 2–3 minutes provide a rough estimate of the duration of the robotic part of the procedure. Observation and waiting times exhibit large variances as well, in agreement

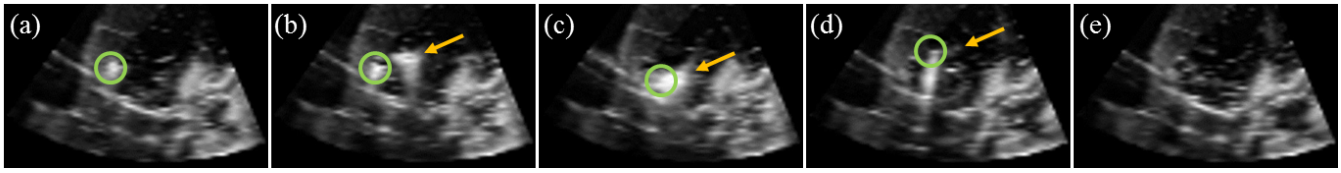

Fig. 5. Foreign body capture sequence. (a) Foreign body (*circle*) in the heart phantom. (b) Robot (*arrow*) approaches capture location. (c) Robot captures foreign body. (d) Robot leaves heart with foreign body. (e) Heart empty after foreign body is extracted.

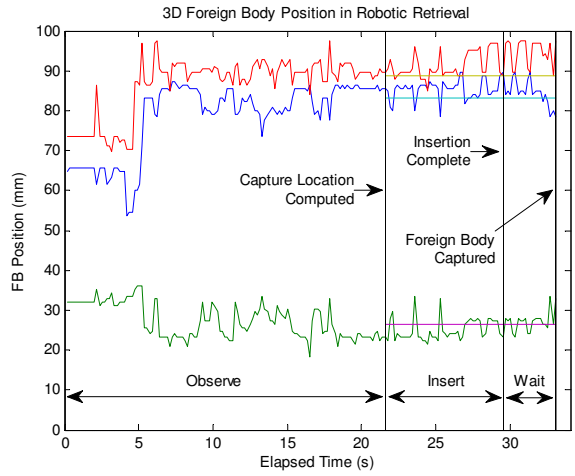

Fig. 6. Example three-axis foreign body motion trace during retrieval, with observation, insertion, and waiting phases annotated.

with previous studies. The variabilities can be attributed to the irregular path of the foreign body, and its tendency to get stuck on occasion, either in a transient pattern of motion or in some area of the heart chamber. Fig. 6 highlights the irregular motion of the foreign body during an example attempt.

E. Comparison of Capture Locations

There was an average distance of 9.1 mm between probability- and dwell time-derived capture locations. We noted this phenomenon previously [10], but the degree of difference is tied to present conditions. For example, in the trivial case in which the foreign body is immobilized, all methods of computing a capture location should be in agreement.

Capture locations based on probability manifested over a range of 8.2 mm, while for dwell time locations this range was 11.7 mm—respectively 22.1% and 31.5% of the average extent of travel (37.1 mm) along the dominant axis. Observation times for probability were lower than for dwell time, with less deviation (Table I, *first row*). There is apparent variability in the dwell time metric, which is more sensitive to particular trajectories. However, waiting times for dwell time were lower and less varying (Table I, *third row*), hinting at a tradeoff between the stability of computing a capture location and of capturing the foreign body there. Thus the preferred method may depend on circumstance. It is also possible that all methods are adequate to the task, especially when readjustment strategies are included.

VI. Conclusions

The adverse symptoms of foreign bodies in the heart must be weighed against the risks of conventional treatment, often a highly invasive surgery. In an effort to improve the state of care, we propose a 3D ultrasound-guided, dexterous robotic system to help surgeons detect and remove foreign bodies from a beating heart in a minimally invasive manner.

In previous work, tracking of a foreign body in a beating heart phantom using streaming 3D TEE was performed. The motion was found to be fast and erratic, and straightforward pursuit using a non-dexterous robot proved difficult. When observed over time, however, distinct tendencies in the motion emerged, offering the possibility of using a slow, dexterous robot to ambush the target at carefully planned capture locations.

In this paper, we introduce a high dexterity robot to test the aforementioned hypothesis. Results of real-time experiments demonstrate the feasibility of the proposed system and approach. With robotic aspects incurring perioperative times on the order of a few minutes, additional observation time can potentially increase robustness and reliability.

We demonstrated near-autonomous capability, but support for a spectrum of cooperative control is a possible future direction. Future work will also address virtual fixtures for protecting heart tissues. Handling different types and multiple foreign bodies are important future tasks. For clinical use, possible future work includes workflow optimization, sterility, capture mechanisms for different types of foreign bodies, and X-ray integration.

Acknowledgment

The authors thank E. Radulescu for insights on ultrasound technology, D. Stanton for support of the heart phantom, and V. Parthasarathy for assistance with the ultrasound equipment. We also thank H. Sen for work on the robot software and I. Iordachita for advice on mechanical components. For their help in the assembly of the snake robot, we thank N. Simaan, K. Xu, and W. Wei.

References

[1] A. J. Marshall, N. J. Ring, and P. L. Newman, "An unexplained foreign body in the myocardium," *J. Royal Society of Medicine*, vol. 95, no. 5, pp. 250–251, May 2002.

[2] P. N. Symbas, A. L. Picone, C. R. Hatcher, and S. E. Vlasis-Hale, "Cardiac missiles. A review of the literature and personal experience," *Annals of Surgery*, vol. 211, no. 5, pp. 639–47; discussion 647–8, May 1990.

[3] Borden Institute, "Ch. 16: Thoracic Injuries," in *Emergency War Surgery: Third United States Revision*, A. C. Szul, L. B. Davis, B. G. Maston, D. Wise, L. R. Sparacino, and J. Shull, Eds. United States Dept. of Defense, 2004, ch. 16, pp. 1–16.

[4] J. C. Williams and W. C. Elkington, "Slow progressing cardiac complications—a case report," *J. Chiropractic Medicine*, vol. 7, no. 1, pp. 28–33, Mar. 2008.

[5] G. M. Actis Dato, A. Arslanian, P. Di Marzio, P. L. Filosso, and E. Ruffini, "Posttraumatic and iatrogenic foreign bodies in the heart: report of fourteen cases and review of the literature," *J. Thoracic and Cardiovascular Surgery*, vol. 126, no. 2, pp. 408–14, Aug. 2003.

[6] J. Evans, L. A. Gray, A. Rayner, and R. L. Fulton, "Principles for the management of penetrating cardiac wounds," *Annals of Surgery*, vol. 189, no. 6, pp. 777–84, June 1979.

[7] Borden Institute, "Ch. 4: Thoracic Trauma," in *War Surgery in Afghanistan and Iraq: A Series of Cases, 2003-2007*, S. C. Nessen, D. E. Lounsbury, and S. P. Hetz, Eds. United States Dept. of Defense, 2008, ch. 4, pp. 118–156.

[8] P. Thienphrapa, H. Elhawary, B. Ramachandran, D. Stanton, and A. Popovic, "Tracking and characterization of fragments in a beating heart using 3D ultrasound for interventional guidance," in *Int. Conf. on Medical Image Computing and Computer-Assisted Intervention (MICCAI)*, Sept. 2011, pp. 211–218.

[9] P. Thienphrapa, B. Ramachandran, R. H. Taylor, and A. Popovic, "A system for 3D ultrasound-guided robotic retrieval of foreign bodies from a beating heart," in *IEEE RAS/EMBS Int. Conf. on Biomedical Robotics and Biomechatronics (BioRob)*, 2012, pp. 743–748.

[10] P. Thienphrapa, B. Ramachandran, H. Elhawary, R. H. Taylor, and A. Popovic, "Multiple capture locations for 3D ultrasound-guided robotic retrieval of moving bodies from a beating heart," in *SPIE Medical Imaging*, vol. 8316, Feb. 2012, p. 831619.

[11] P. Thienphrapa, A. Popovic, and R. H. Taylor, "3D ultrasound-guided retrieval of foreign bodies from a beating heart using a dexterous surgical robot," in *Hamlyn Symposium on Medical Robotics*, 2013.

[12] J. Stoll, P. Novotny, R. Howe, and P. Dupont, "Real-time 3D ultrasound-based servoing of a surgical instrument," in *IEEE Int. Conf. on Robotics and Automation (ICRA)*. IEEE, 2006, pp. 613–618.

[13] P. Novotny, J. Stoll, P. Dupont, and R. Howe, "Real-time visual servoing of a robot using three-dimensional ultrasound," in *IEEE Int. Conf. on Robotics and Automation (ICRA)*. IEEE, 2007, pp. 2655–2660.

[14] K. Liang, D. V. Allmen, A. J. Rogers, E. D. Light, and S. W. Smith, "Three-dimensional ultrasound guidance of autonomous robotic breast biopsy: feasibility study," *Ultrasound in Medicine & Biology*, vol. 36, no. 1, pp. 173–7, 2010.

[15] S. G. Yuen, D. T. Kettler, P. M. Novotny, R. D. Plowes, and R. D. Howe, "Robotic motion compensation for beating heart intracardiac surgery," *Int. J. Robotics Research*, vol. 28, no. 10, pp. 1355–1372, May 2009.

[16] S. Kesner, S. Yuen, and R. Howe, "Ultrasound servoing of catheters for beating heart valve repair," in *Information Processing in Computer-Assisted Interventions (IPCAI)*, N. Navab and P. Jannin, Eds. Geneva, Switzerland: Springer Berlin Heidelberg, 2010, pp. 168–178.

[17] A. Krupa, G. Fichtinger, and G. D. Hager, "Real-time motion stabilization with B-mode ultrasound using image speckle information and visual servoing," *Int. J. Robotics Research*, vol. 28, no. 10, pp. 1334–1354, Oct. 2009.

[18] R. Mebarki, A. Krupa, and F. Chaumette, "Modeling and 3D local estimation for in-plane and out-of-plane motion guidance by 2D ultrasound-based visual servoing," in *IEEE Int. Conf. on Robotics and Automation (ICRA)*. IEEE, 2009, pp. 319–325.

[19] M.-A. Vitrani, H. Mitterhofer, N. Bonnet, and G. Morel, "Robust ultrasound-based visual servoing for beating heart intracardiac surgery," in *IEEE Int. Conf. on Robotics and Automation (ICRA)*, vol. 13, no. 5. IEEE, 2007, pp. 3021–3027.

[20] M. Sauvee, P. Poignet, and E. Dombre, "Ultrasound image-based visual servoing of a surgical instrument through nonlinear model predictive control," *Int. J. Robotics Research*, vol. 27, no. 1, pp. 25–40, Jan. 2008.

[21] P. Abolmaesumi, S. Salcudean, W. Zhu, M. Sirouspour, and S. DiMaio, "Image-guided control of a robot for medical ultrasound," *IEEE Transactions on Robotics and Automation*, vol. 18, no. 1, pp. 11–23, 2002.

[22] E. Boctor, G. Fischer, M. Choti, G. Fichtinger, and R. H. Taylor, "A dual-armed robotic system for intraoperative ultrasound guided hepatic ablative therapy: a prospective study," in *IEEE Int. Conf. on Robotics and Automation (ICRA)*, vol. 3. IEEE, 2004, pp. 2517–2522.

[23] A. Rogers, E. Light, and S. Smith, "3-D ultrasound guidance of autonomous robot for location of ferrous shrapnel," *IEEE Transactions on Ultrasonics, Ferroelectrics, and Frequency Control*, vol. 56, no. 7, pp. 1301–3, 2009.

[24] M. Fronheiser, S. Idriss, P. Wolf, and S. Smith, "Vibrating interventional device detection using real-time 3-D color Doppler," *IEEE Transactions on Ultrasonics, Ferroelectrics, and Frequency Control*, vol. 55, no. 6, pp. 1355–62, 2008.

[25] J. T. Moore, M. W. A. Chu, B. Kiaii, D. Bainbridge, G. Guiraudon, C. Wedlake, M. Currie, M. Rajchl, R. V. Patel, and T. M. Peters, "A navigation platform for guidance of beating heart transapical mitral valve repair," *IEEE Transactions on Biomedical Engineering*, vol. 60, no. 4, pp. 1034–40, Apr. 2013.

[26] A. H. Gosline, N. V. Vasilyev, E. J. Butler, C. Folk, A. Cohen, R. Chen, N. Lang, P. J. del Nido, and P. E. Dupont, "Percutaneous intracardiac beating-heart surgery using metal MEMS tissue approximation tools," *Int. J. Robotics Research*, pp. 1081–1093, May 2012.

[27] B. Ramachandran, P. Thienphrapa, A. Jain, and A. Popovic, "Tracking using 3D ultrasound for guiding cardiac interventions," in *Int. Conf. on Biomedical Engineering*, 2011.

[28] K. L. Ryan, W. H. Cooke, C. A. Rickards, K. G. Lurie, and V. A. Convertino, "Breathing through an inspiratory threshold device improves stroke volume during central hypovolemia in humans," *J. Applied Physiol. (Bethesda, Md. 1985)*, vol. 104, no. 5, pp. 1402–9, May 2008.

[29] J. B. Kostis, E. Mavrogeorgis, A. Slater, and S. Bellet, "Use of a range-gated, pulsed ultrasonic Doppler technique for continuous measurement of velocity of the posterior heart wall," *Chest*, vol. 62, no. 5, p. 597, Nov. 1972.

[30] N. Simaan, R. H. Taylor, and P. Flint, "A dexterous system for laryngeal surgery," in *IEEE Int. Conf. on Robotics and Automation (ICRA)*. IEEE, 2004, pp. 351–357.

[31] A. Kapoor, N. Simaan, and P. Kazanzides, "A system for speed and torque control of DC motors with application to small snake robots," in *IEEE Int. Conf. on Mechatronics and Robotics (MechRob)*, 2004.

[32] N. Simaan, R. H. Taylor, and P. Flint, "High dexterity snake-like robotic slaves for minimally invasive telesurgery of the upper airway," in *Int. Conf. on Medical Image Computing and Computer-Assisted Intervention (MICCAI)*, ser. Lecture Notes in Computer Science, C. Barillot, D. Haynor, and P. Hellier, Eds., vol. 3217. Springer Berlin Heidelberg, 2004, pp. 17–24.

[33] A. Kapoor, "Motion constrained control of robots for dexterous surgical tasks," Ph.D. dissertation, Johns Hopkins Univ., Sept. 2007. [Online]. Available: http://search.proquest.com/docview/304616212

[34] N. Simaan, K. Xu, W. Wei, A. Kapoor, P. Kazanzides, R. H. Taylor, and P. Flint, "Design and integration of a telerobotic system for minimally invasive surgery of the throat," *Int. J. Robotics Research*, vol. 28, no. 9, pp. 1134–1153, 2009.

[35] R. H. Taylor, J. Funda, B. Eldridge, S. Gomory, K. Gruben, D. LaRose, M. Talamini, L. Kavoussi, and J. Anderson, "A telerobotic assistant for laparoscopic surgery," *IEEE Engineering in Medicine and Biology Magazine*, vol. 14, no. 3, pp. 279–288, 1995.

[36] P. Thienphrapa and P. Kazanzides, "Design of a scalable real-time robot controller and application to a dexterous manipulator," in *IEEE Int. Conf. on Robot. and Biomimetics (ROBIO)*, 2011, pp. 2295–2300.

[37] J. Funda, R. H. Taylor, B. Eldridge, S. Gomory, and K. Gruben, "Constrained Cartesian motion control for teleoperated surgical robots," *IEEE Transactions on Robotics and Automation*, vol. 12, no. 3, pp. 453–465, June 1996.

[38] A. Kapoor, M. Li, and R. H. Taylor, "Constrained control for surgical assistant robots," in *IEEE Int. Conf. on Robotics and Automation (ICRA)*, 2006, pp. 231–236.

[39] P. Thienphrapa, B. Ramachandran, H. Elhawary, A. Popovic, and R. H. Taylor, "Intraoperative analysis of locations for 3D ultrasound-guided capture of foreign bodies from a beating heart," in *Hamlyn Symposium on Medical Robotics*, 2012.